CHEMICAL ENGINEERING TRANSACTIONS
VOL. 41, 2014
A publication of AIDIC
The Italian Association of Chemical Engineering
www.aidic.it/cet
Guest Editors: Simonetta Palmas, Michele Mascia, Annalisa Vacca

ISBN 978-88-95608-32-7; **ISSN** 2283-9216
DOI: 10.3303/CET1441064

Photo-Electrochemical Properties of WO_3 and α-Fe_2O_3 Thin Films

J. Krysa [a]*, M. Zlamal[a], S. Kment[b] and Z. Hubicka[b]

[a] Institute of Chemical Technology Prague, Technicka 5, 16628 Prague, Czech Republic
[b] Institute of Physics, Academy of Sciences of the Czech Republic, Na Slovance 2, 14800 Prague, Czech Republic]
*josef.krysa@vscht.cz

Iron oxide (α-Fe_2O_3) in hematite crystalline structure and tungsten trioxide have recently attracted much attention as possibly convenient materials to be used for hydrogen production via photoelectrochemical water splitting. Thius is due to their favorable properties such as band gaps between 2.0 - 2.2 eV (α-Fe_2O_3) and 2.5–2.8 eV (WO_3) which allows absorbing of a substantial fraction of solar spectrum. FTO glass substrates were used for both types of films. Tungsten trioxide films were prepared by sedimentation of WO_3 particles and further annealing at different temperatures to improve adhesion. Iron oxide (α-Fe_2O_3) hematite films were prepared by advanced pulsed plasma deposition method of High Power Impulse Magnetron Sputtering (HiPIMS). The films were evaluated on the basis of physical properties such as crystalline structure, surface topography and electrical behavior. The functional properties were investigated under simulated photoelectrochemical (PEC) water splitting conditions. Different excitation lights were used: monochromatic (very narrow single peak at light spectra) and the standard solar illumination conditions (AM 1.5 G). Also the influence of the electrolyte/electrode and substrate/electrode illumination of layers was studied. As deposited WO_3 films have rather small photocurrents. Higher annealing temperature results in better adhesion of particles and increase in photocurrent. Optimum annealing temperature is 450-500 ºC. Increase of the annealing temperature to 600 °C caused the formation of undesirable crystal phases (produced by the reaction of WO_3 and FTO layer) and significant decrease in photocurrent. Despite confirmed hematite phase of as-deposited films, these were almost photoelectrochemically inactive. The main reason is probably the high density of defects and imperfections in crystalline structure, and thus a high extend of backward electron-hole pair recombination. Annealing in air at 650 °C significantly improved photoefficiency which can be explained by the diffusion of tin from the FTO substrate into hematite resulting in the extrinsic doping of hematite improving its electronic properties.

1. Introduction

Tungsten trioxide is widely used for photocatalytic experiments, especially for those using visible light. It is an indirect band gap semiconductor (Eg ~ 2.5–2.8 eV) that can capture approximately 12% of the solar spectrum and can absorb light in the visible spectrum up to 500 nm (Sun et al. 2009). It is also convenient material to be used for hydrogen production via photoelectrochemical water splitting (Liu et al. 2012). Layers formed by particles of material have the advantage of relatively high specific surface area usable for the reactions. But the mechanical stability and conductivity of these layers are very low due to weak adhesion of the particles. Both can be improved by layer calcination.
Iron oxide (α-Fe_2O_3) in hematite crystalline structure has recently attracted much attention as a possibly convenient material to be used for hydrogen production via photoelectrochemical water splitting. It is due to its favorable properties such as a band gap between 2.0 - 2.2 eV, which allows absorbing a substantial fraction of solar spectrum, chemical stability in aqueous environment, nontoxicity, abundance, and low cost. For such band gap and assuming the standard solar illumination conditions (AM 1.5 G, 100 mW cm^{-2}) theoretical maximal solar-to-hydrogen (STH) conversion efficiency can be calculated as 15 % (Sivula et al. 2011). However not everything is ideal and hematite possesses also certain disadvantages. Among the most cited limitations are: the nonideal position of hematite's conduction band, which is too low for spontaneous water reduction (can be addressed by applying e.g. a PV cell to provide the additional energy needed); the low absorptivity (especially for longer wavelengths); and very short diffusion length of

Please cite this article as: Krysa J., Zlamal M., Kment S., Hubicka Z., 2014, Photo-electrochemical properties of wo3 and alpha-fe2o3 thin films, Chemical Engineering Transactions, 41, 379-384 DOI: 10.3303/CET1441064

photogenerated holes. This creates a disaccord between the depth where charge carriers are photogenerated (in the bulk) and the distance they diffuse before recombining. Doping with elements such as Sn, Ti, Ge, Si, Nb, etc. can significantly increase the electronic conductivity by increasing the number of carriers. The negative effect of the short diffusion length of holes can be suppressed by using very thin films of hematite or their nanostructuring. Furthermore, the remarkable overpotential of about 0.4 – 0.6 V for the onset of the water splitting photocurrent, which has been assigned to poor oxygen evolution kinetics on hematite surfaces and/or to the presence of surface defects acting as traps, is another crucial issue.
The aim of the present work was the comparison of WO_3 and hematite thin films with respect to their utilisation as anodes in an photoelectrochemical cell for water splitting. WO_3 films were fabricated from powder WO_3 particles by sedimentation and thermal annealing. Hematite thin films were prepared by means of novel plasma-assisted deposition technique of High Power Impulse Magnetron Sputtering (HiPIMS). The HiPIMS discharges are operated in pulse modulated regime with a low repetition frequency (typically about 100 Hz) and a short duty cycle (~1 %) with applying high peak powers (~ kW/cm^2) during the active part of the modulation cycle (Lundin, Sarakinos 2012). A distinguishing feature of HiPIMS is its high degree of ionization of the sputtered metal and a high rate of molecular gas dissociation due to very high plasma density near the target (order of 10^{13} ions cm^{-3}). Some of the above mentioned drawbacks of hematite working as a photoanode in a photoelectrochemical cell (PEC) simulating the water splitting conditions were addressed in this study by deposition of very thin films of hematite (25 nm) and by doping the hematite with Sn.

2. Experimental

Film preparation
Tungsten trioxide films were prepared from commercial powder (99 % WO_3, Fluka) by the sedimentation method. The material has relatively big aggregates and it was not possible to produce a stable suspension, so it was ground by agate mortar and pestle. Ground material was mixed with distilled water to obtain a suspension with a known concentration of WO_3. Before application of the suspension on FTO glass (TCO22-15, Solaronix) the suspension was ultrasonicated for 10 minutes. Substrate slides had dimensions of 1x5 cm and after application of the suspension were dried at 60 °C and then thermally annealed at 300, 400, 450, 500 and 600 °C for 2 hours.
Hematite films were prepared by advanced pulsed plasma deposition method of HiPIMS. The HiPIMS deposition employed a metallic target of pure iron (99.995 %, Plasmaterials) with outer diameter 50 mm and an Ar-O_2 atmosphere as working gas mixture in an ultra-high vacuum (UHV) reactor continuously pumped down by a turbo-molecular pump providing the base pressure of 10^{-5} Pa. As the substrates were used carefully cleaned fused-silica (SiO_2) and fluorine-doped tin oxide (FTO, TCO-7, Solaronix) and the deposition was carried out at room temperature. The working gases were fed to the reactor with the flow rates of 30 sccm (standard cubic centimeters per minute) and 12 sccm corresponding to argon and oxygen, respectively. The operating pressure of 1 Pa was set. The pulsing frequency of DC HiPIMS discharge was in the range 70-1000 Hz with the “ON” time of 100 μs and the maximal current density achieved in a pulse was 5 ≈ Acm^{-2} at 70 Hz (Hubicka et al. 2013).

Film characterization
The structural, morphological, electronic and optical properties of the deposited films were determined using X-ray diffraction (XRD), SEM, AFM and space resolved Raman spectroscopy. Photo-electrochemical measurements were done in glass cell with three-electrode arrangement. The irradiated surface area of each sample was set to 1 cm^2 by a teflon tape, a Pt plate was used as counter electrode and Ag/AgCl as reference electrode. The cell was connected to the potentiostat (PGZ100, VoltaLab) and situated at the end of an optical bench consisting of the light source, infrared filter, bandpass filter and PC-controlled shutter. Two types of light sources were used: solar simulator – 150 W Xe arc lamp (Newport) with AM1.5G filter and 500 W Hg arc lamp (Lot-Oriel) with 315, 365 and 404 nm bandpass filters. Intensities of used lights entering the cell were 1 mW/cm^2 for 315, 365 nm, 10 mW/cm^2 for 404 nm, and 1 sun (1000 W/m^2) simulating the standard solar illumination conditions.
Linear voltammetry of WO_3 and α-Fe_2O_3 layers was measured while periodically illuminated (5 s light/5 s dark) and irradiated from the electrolyte/electrode (EE) and from the substrate/electrode (SE) interface. 0.1 M sodium sulphate (WO_3) and 1 M sodium hydroxide (α-Fe_2O_3) were used as electrolytes.
For the straightforward comparison of both films using solar AM 1.5G light the measured potentials vs Ag/AgCl were converted to the reversible hydrogen electrode (RHE) scale according to the Nernst equation:

$$E_{RHE} = E_{Ag/AgCl} + 0.059\,pH + E^0_{Ag/AgCl} \quad (1)$$

where E_{RHE} is the converted potential vs. RHE, $E°_{Ag/AgC}$ is 0.205 V at 25 °C, and $E_{Ag/AgCl}$ is the experimentally measured potential against Ag/AgCl reference electrode.

3. Results and Discussion

3.1 WO_3 films

XRD diffraction patterns of WO_3 powder and WO_3 films (0.1 mg/cm^2) deposited on FTO substrate and calcined at 300, 450 and 600 °C are shown in Figure 1. Table 1 then summarises the identified crystalline phases and corresponding diffraction angles. The crystalline structure of WO_3 particles is difficult to identify. Reference XRD data for monoclinic, triclinic and orthorhombic crystalline structure are almost identical and do not help in the identification. Due to the relatively small thickness, WO_3 films show only bands with the highest relative intensity (diffraction angles 2Θ = 22.92, 24.23, 28.56, 33.05, 33.60, 34.00 and 50.10°). There are also 4 bands (diffraction angles 2Θ = 26.58, 37.77, 51.76 and 65.74°) corresponding to the fluorine doped SnO_2 layer. Calcination at 300 and 500 °C does not influence the crystalline structure of WO_3 particles in the film. But after calcination at 600 °C several bands corresponding to WO_3 disappears and new bands corresponding to $Na_2W_3O_{10}$ and $SnWO_4$ appears in XRD diffraction patterns. This means that at this temperature WO_3 reacts with SnO_2 in the FTO layer on the glass substrate and also with Na penetrating from the glass substrate at 600 °C.

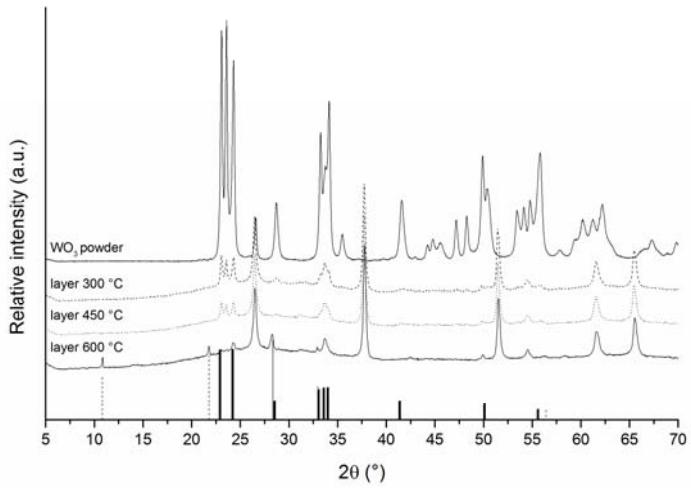

Figure 1 XRD of WO_3 powder and film on FTO substrate calcined at various temperatures

Table 1. List of identified crystalline phases and corresponding diffraction angles

2Θ/	Phase	Line
10.84	$Na_2W_3O_{10}$	dotted
21.81	$Na_2W_3O_{10}$	dotted
22.92	WO_3	bold
24.23	WO_3	bold
28.36	$SnWO_4$	solid
28.56	WO_3	bold
32.97	$Na_2W_3O_{10}$	dotted
33.05	WO_3	bold
33.60	WO_3	bold
34.00	WO_3	bold
41.40	WO_3	bold
50.10	WO_3	bold
55.61	WO_3	bold
56.43	$Na_2W_3O_{10}$	dotted

Polarization curves of the WO_3 particle layer under chopped light (Figure 2) showed increasing photocurrents at the potential interval from 0 V to 0.5 V (vs. Ag/AgCl) and typical plateau from 0.5 to 1.5 V (vs. Ag/AgCl). Further increase of the potential leads to steep increase of dark current, which indicates electrochemical evolution of oxygen on the sample.

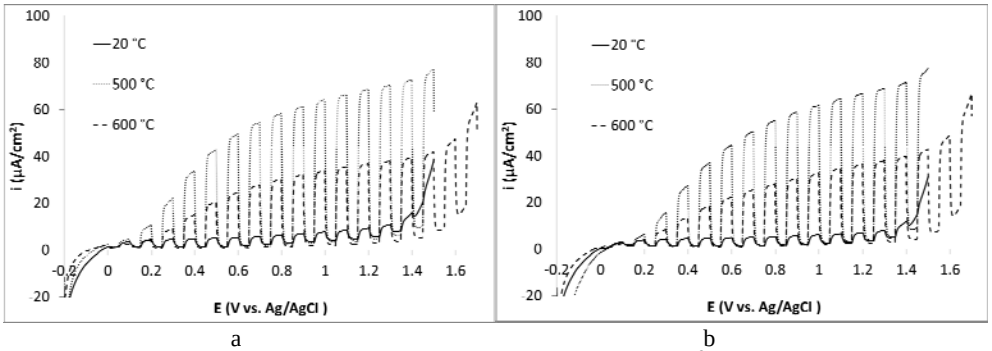

Figure 2 Chopped light polarization curve on WO_3 films (0.1 mg/cm^2) in 0.1 M Na_2SO_4, 365 nm, 1 mW/cm^2. a) EE irradiation, b) SE irradiation

Photocurrents measured at 1 V (vs. Ag/AgCl) and corresponding values of IPCE (incident photon to current efficiency) were used for direct comparison of the prepared layers. IPCE was calculated using the

relation:

$$IPCE = \frac{j}{F\,P} \qquad (2)$$

where j is the photocurrent density [A cm^{-2}], F is the Faraday constant (96.485 C mol^{-1}) and P is the incident light intensity at wavelength corresponding to particular monochromatic irradiation [Einstein cm^{-2} s^{-1}]. Figure 3 shows the dependence of IPCE on calcination temperature at three irradiation wavelengths. The highest IPCE values were achieved for annealing temperature 500 °C. But increase of annealing temperature to 600 °C resulted in the decrease of IPCE. This could be explained by the formation of new crystal phases at the interface of the FTO layer and WO_3 layer, $SnWO_4$ and $Na_2W_3O_{10}$, which were detected by XRD (see Figure 1). These phases probably figure as insulating material and block migration of the electrons from WO_3 to FTO layer. The dependence of IPCE on annealing temperature has a similar trend for all three wavelengths. As expected IPCE increases with wavelength from 404 to 315 nm. Lower IPCE generated by 404 nm light is caused by smaller amount of light absorbed by WO_3 at this wavelength. From measured transmittance and reflectance of the WO_3 layer we can calculate that such layer absorbs 45, 28 and 11 % of light at 315, 365 and 404 nm, respectively.

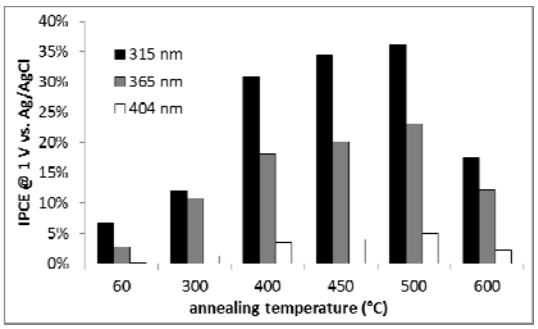

Figure 3. Values of IPCE at potential 1 V (Ag/AgCl) at corresponding wavelengths for WO_3 particulate layer calcined at various temperatures, irradiation form the EE interface.

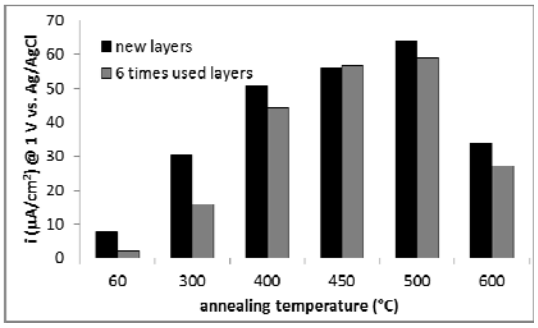

Figure 4. Repeatability of photocurrent on WO_3 particulate layers irradiated from the EE interface by monochromatic light, 365 nm, 1 mW/cm^2.

The photocurrent on WO_3 films was measured repeatedly and Figure 4 shows the initial value of photocurrent and the value after six repeated measurements. It ca be seen that the stability of layers which were not thermally annealed was very low. Every electrochemical measurement causes loss of particles from the layer and photocurrent decrease with increasing number of measurement (to 20% of initial value). Calcination of layers at 300 °C improves the stability in comparison with non-annealed layer, but photocurrents of such sample still decreases to 50 % (of initial value) after six measurements. Increase of the annealing temperature to 400-500 °C improves the stability of particle layers significantly.

3.2 Fe_2O_3 films

Due to the very small thickness of Fe_2O_3 films the crystalline structure of as-deposited samples was assessed by Raman spectroscopy (Figure 5). The Raman spectrum denotes that the hematite crystalline phase was achieved already during the depositions. The database hematite spectrum is presented for reference and it unambiguously matches the measured HiPIMS Raman spectra. With the help of AFM the surface morphology of the films was visualized (inset of Figure 5). From the captured images it was clearly seen that the HiPIMS films consist of very small densely packed particles. Nevertheless, such organizations are a common feature of HiPIMS produced thin films in general. The measured surface RMS

roughness was only ~ 2 nm for the HiPIMS films. The indirect band gap energy width of 1.99 eV, which is from the region of the theoretical values, was estimated based on a Tauc plot.

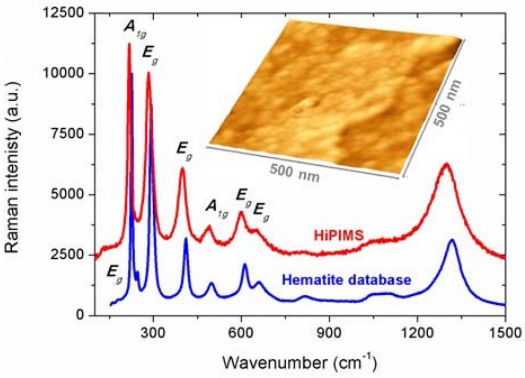

Figure 5. Raman spectra and AFM surface image (insert) of as-deposited HiPIMS hematite thin films.

Figure 6 shows photoelectrochemical performance of hematite films under conditions simulating PEC water splitting. As stated in the introduction the hematite films struggle with short diffusion length of the holes. Hence in order to moderate this drawback the very thin films of 25 nm were fabricated for PEC water splitting. Although the as-deposited films were crystalline, they behaved almost inactive in the PEC system. The high density of defects and imperfections in crystalline structure, and thus a high extent of backward electron-hole pair recombination of as-deposited hematite films, is probably the main reason for the poor photoactivity.

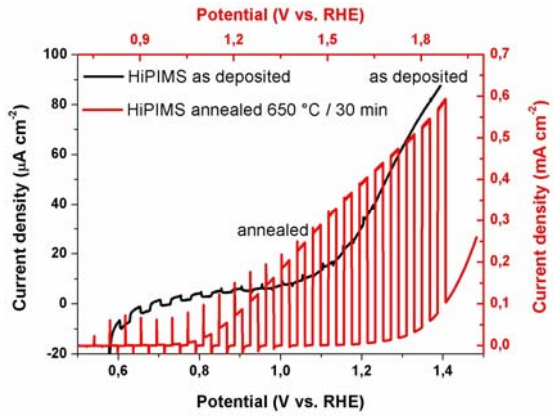

Figure 6. Chopped light polarization curve of the as-deposited and annealed (650 °C/ 30 min) hematite films, 1 M NaOH, irradiation AM 1.5G.

Thus, in the next step the films were annealed in air at 650 °C for 30 min. It is already known that such a high temperature is needed for the diffusion of tin from the FTO substrate into hematite to occur. The diffused tin ions provide for the extrinsic doping of hematite improving its electronic properties (Sivula et al. 2010). A considerable increase of the photoactivity is evident - 0.09 $mAcm^{-2}$ at 1.23 V vs. RHE. One of the positive effect of HiPIMS method enhancing the photefficiency is apparently related to a very high energy of ions and sputtered particles (can be higher than 20 eV (Bohlmark et al. 2006)) bombarding the substrate during the deposition by means of HiPIMS. As a consequence the interface and electrical conductivity between the FTO and hematite film is significantly boosted. Second reason for the increased photoactivity of HiPIMS is apparently attributed to the much smaller grains, which are beneficial for the process in terms of reduced electron-hole recombination due to optimal matching of nanoparticle size with the hole diffusion length (Sivula et al. 2011).

3.3 Comparison of WO_3 and Fe_2O_3 films

Comparison of both films regarding PEC water splitting is shown in Figure 7. In the case of WO_3 film photocurrent starts to increase already at about 0.7 V. At 1.2 V the increase is slower and photocurrent reaches a plateau with a value around 130 $\mu A/cm^2$ at 1 V (vs. RHE) and 240 $\mu A/cm^2$ at 1.7 V (vs. RHE).

At potential 2.1 V then starts to increase also dark current. In the case of Fe_2O_3 films photocurrent starts to increase at more positive potential (about 1.1 V) and then almost linearly increases with potential with value around 350 μA/cm^2 at 1.5 V (vs. RHE) and 480 μA/cm^2 at 1.7 V (vs. RHE). Dark current starts to increase at potential 1.7 V vs. RHE. It would mean that WO_3 films generate photocurrent at lower values of potential where Fe_2O_3 shows no photocurrent. On the other side at potential 1.7 V (vs. RHE) Fe_2O_3 exhibits two times higher photocurrent than WO_3.

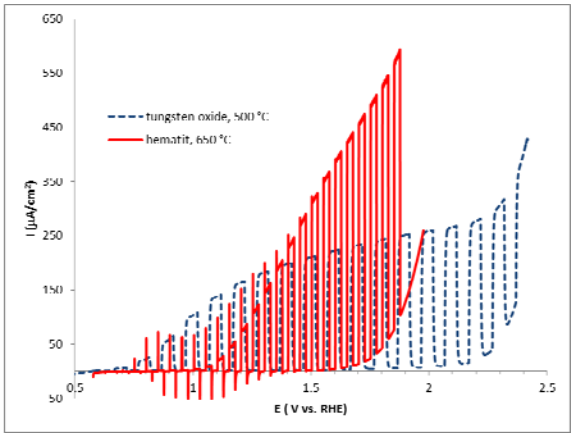

Figure 7. Comparison of PEC behaviour of tungsten oxide and hematite films, irradiation AM 1.5G.

4. Conclusions

Annealing of deposited particulate WO_3 films at temperatures 450-500 ºC results in better adhesion of particles to the FTO substrate and significant increase in photocurrent. Annealing at 600 °C caused the formation of undesirable crystal phases and significant decrease in photocurrent. Deposited hematite films were almost photoelectrochemically inactive but annealing in air at 650 °C significantly improved photocurrent; this can be explained by the diffusion of tin from the FTO substrate into hematite.
Comparison of both films using irradiation AM 1.5 G. results in two times higher photocurrent for Fe_2O_3 film (at 1.7 V vs. RHE) but, on the other hand, the WO_3 film exhibits photocurrent already at 1 V (vs. RHE) where photocurrent at the Fe_2O_3 film is negligible.

Acknowledgement
This work was supported by the Grant Agency of the Czech Republic (P108/12/2104).

References

Bohlmark J., Lattermann M., Gudmundsson J.T., Ehiasarian A.P., Aranda Gonzalvo Y., Brenning N., Helmersson U., 2006, The ion energy distributions and ion flux composition from a high power impulse magnetron sputtering discharge, Thin Solid Films, 515, 1522-1526.

Hubicka Z., Kment S., Olejnicek J., Cada M., Kubart T., Brunclikova M., Ksirova P., Adamek P., Remes Z., 2013 Deposition of hematite Fe2O3 thin film by DC pulsed magnetron and DC pulsed hollow cathode sputtering system, Thin Solid Films, 549, 184-191.

Liu X., Wang F., Wang Q., Nanostructure-based WO_3 photoanodes for photoelectrochemical water splitting, 2012, Phys. Chem. Chem. Phys., 14, 7894-7911.

Lundin D., Sarakinos K., An introduction to thin film processing using high-power impulse magnetron sputtering, 2013, Journal Materials Research, 27, 780-792.

Sivula K., Zboril R., Le Formal F., Robert R., Weidenkaff A., Tucek J., Frydrych J., Gratzel M., 2010, Photoelectrochemical Water Splitting with Mesoporous Hematite Prepared by a Solution-Based Colloidal Approach, Journal of the American Chemical Society, 132, 7436-7444.

Sivula K., Le Formal F., Grätzel M., Solar Water Splitting: Progress Using Hematite (α-Fe2O3) Photoelectrodes, 2011, Chem. Sus. Chem, 4, 432-449.

Sun Y., Murphy C.J., Reyes-Gil K.R., Reyes-Garcia E.A., Tornton J.M., Morris N.A., Raftery D., 2009, Photoelectrochemical and structural characterization of carbon-doped WO_3 films prepared via spray pyrolysis, Int. Journal of Hydrogen Energy, 34, 8476-8484.